Asian Journal of Scientific Research

ISSN 1992-1454

science alert
http://www.scialert.net

ANSInet
an open access publisher
http://ansinet.com

Asian Journal of Scientific Research 1 (1): 22-31, 2008
ISSN 1992-1454

Consolidation of WC-Ni/W-Ni Double-Layer Composite by Infiltration of Cu-Sn-Ni-Mn as Binder in SILP Process

D. Miroud, M. Tata and S. Lebaili
Laboratoire de Science et Génie des Matériaux,
Faculté de Génie Mécanique et Génie des Procédés,
Université des Sciences et de la Technologie Houari Boumédien,
USTHB, BP32-16111 El Alia, Bab Ezzouar, Alger, Algérie

Abstract: In this study, two layers of loose powders' mixtures (WC-15% Ni and W-14% Ni) are consolidated by the infiltration of a nickel bronze alloy (Cu-6% Sn-9% Ni-5% Mn) to form a double-layer composite. We varied the granulometry of the powders in four classes. We are particularly interested in the densification at the level of the formed interfaces *in situ* on the basis of interactions between the binder and the mixtures of powders as well as in the effect of certain elements on the formed composite cohesion. Hardness profiles are established in the direction of the infiltration and microhardness tests on the phases resulting from solidification will consolidate the various microstructural observations.

Key words: Infiltration, SILP process, double-layer composite, interfaces

INTRODUCTION

The composites with two matrices (double-layered) are very useful under the conditions of wear and corrosion (Eremenko *et al*., 1970). They are composed by the contact zone of WC-Ni with a high volume of hard phase and a low volume of binder and a tougher zone made up of a matrix W-Ni. The properties of these composites are given as well by the hard particles as by the metal binder. They vary according to the proportions of WC, W and Ni, to the size of the particles and their distribution, in particular in the interface, as well as elements of addition (Shatov *et al*., 1998; Gille *et al*., 2000). A better densification is observed with fine particles and a fast rate of heating (German, 1985; Miroud *et al*., 2001).

The unconventional sintering process by infiltration of appropriate mixture with loose powders (SILP) constitutes the ouly technique to carry out large-sized elements having a complex geometry-tool set with diamonds intended to oil and mining drilling, resistant to erosion and abrasion with weak tension- (Orban and Domsa, 1999; Domsa and Orban, 1999; Thibault *et al*., 1999). This process allows a better dimensional check and an porosity elimination for the mixture of powders having a very low compressibility and a nil green resistance (German, 1987).

As defined in the specific processes of sintering, the conventional infiltration is used to increase the density by the introduction of a metal in the liquid state into the pre-sintered compressed process, by contact (Goetzel and Shaler, 1964; Chong *et al*., 1993; Wannasin and Flemings, 2005; Abd-Elwahed, 1999), by gravity-feed infiltration (Goetzel and Shaler, 1964), under vacuum or pressure (Cook and Werner, 1991). Under the effect of the capillary forces, the introduced molten metal fills the system of inter-connected pores forming a rigid skeleton resulting from the operation of compaction (Thibault *et al*., 1999; German, 1987; Goetzel and Shaler, 1964). The structure resulting from this process is similar to that obtained by sintering in liquid phase (Caceras, 2002; Ashurst, 1983; Kumar and Kruth, 2007).

Corresponding Author: D. Miroud, Laboratoire de Science et Génie des Matériaux,
Faculté de Génie Mécanique et Génie des Procédés,
Niversité des Sciences et de la Technologie Houari Boumédien, USTHB,
BP32-16111 El Alia, Bab Ezzouar, Alger, Algérie Fax: (21321)515028

The various studies available on the phenomenon of sintering in liquid phase by infiltration (Orban and Domsa, 1999; Domsa and Orban, 1999; German, 1985) described the microstructural evolution like a process which can take place without substantial shrinkage, in which the inter-connected pores of the packed free powders are filled with a metal or alloy with a low melting point. This process is similar to sintering in liquid phase where one of the components melts in-situ and filled the pores by shrinkage and particles rearrangement. The total reduction of the surface free energy of the system is prerequired during the infiltration. With atmospheric pressure, the surface tension and the difference in pressure in the pores are the driving forces of infiltration (Shaler, 1965). Capillary attraction becomes the driving force of the infiltration inducing a reduction of interfacial energy if the infiltrating pellets (binder) melt slowly (Orban and Domsa, 1999).

In this study, two layers of powders' mixtures (the matrices WC-15% Ni and W-14% Ni), are consolidated by the infiltration of a nickel bronze alloy (Cu-6% Sn-9% Ni-5% Mn-1% Fe) to form a double-layer composite. For the same conditions of infiltration we varied the granulometry of the powders in four classes. We are particularly interested in the densification at the level of the formed interfaces *in situ* on the basis of interactions between the binder and the mixtures of powders as well as in the effect of certain elements on the formed composite cohesion. Hardness profiles are established in the direction of the infiltration. Microhardness tests on the phases resulting from solidification will consolidate the various microstructural observations.

MATERIALS AND METHODS

Mixtures and Powder Classes

Each composite consists of two layers of homogeneous mixtures, LP1 (W-15% Ni) and LP2 (WC-15% Ni), prepared from W, WC and Ni pure powders (as received from PTD/ENSP-Algeria). Figure 1 shows the morphological aspect of these powders and Table 1 summarizes their characteristics.

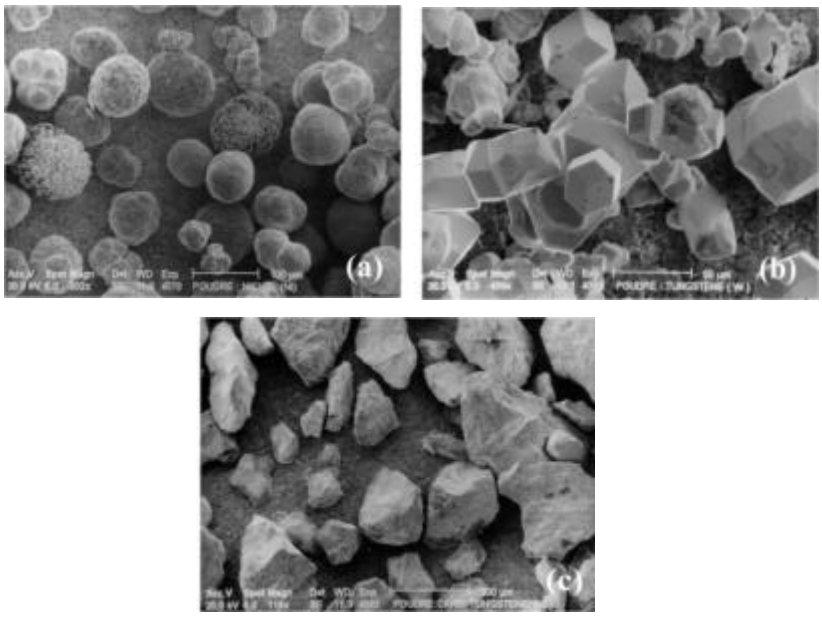

Fig. 1: MEB microstructures showing the morphology of the used pure powders. Sphaero-granular Nickel a, Polygonal form tungsten b and tungsten carbide irregular morphology c

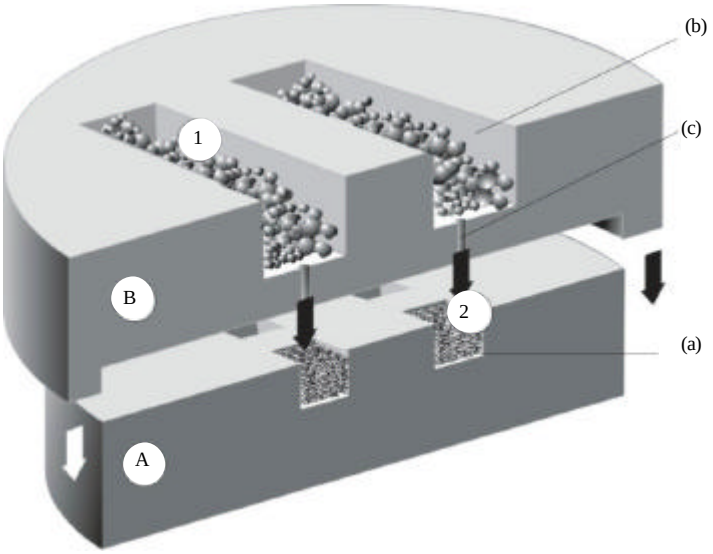

Fig. 2: Infiltration mould

Table 1: Characteristics of the basic powder used

Powder	Purity (%)	Manufacturing method	Form	Density (g cm^{-3}) Theoretical	Apparent	tap	BET ($m^2 g^{-1}$)
W	99.5	Chemical reduction	Polygonal	19.3	6.6	7.8	0.0330
Ni	99.7	Carbonyl decomposition	Granulo-spherical	8.9	4.5	5.1	0.0291
WC	95.7	-	irregular	-	7.6	8.9	0.0397

In order to discuss the size and distribution effect of the powders in the process of infiltration, four classes of mixtures are carried out: C_1 (38-75 μm), C_2 (75-106 μm), C_3 (106-212 μm) and C_4 (44-250 μm for LP1 and 74-500 μm for LP2). The size of the Ni particles does not exceed 149 μm for the two mixtures and all the classes.

The samples are carried out in a graphite mould by gravity infiltration technique (Fig. 2). 10×10×10 mm^3 rectangular prints (a) are machined in 50 mm thickness part. For all classes, LP1 and LP2 mixtures are superimposed in the prints, respectively with 45 and 65% proportions. The porosity wished in the mixtures is obtained by vibrations during the filling. The capillary forces are increased by the external pressure being exerted from a tank (B) of infiltrating liquid placed in top on part (A). It will be used to contain the granules (b) of binder which at the time of its fusion will feed with sufficient quantities in the prints thus prepared. The separation of the tank of the mixtures is ensured by a vertical channel (c) to avoid the effect of erosion. The infiltration process being very sensitive to the contamination on the surface, the volatile impurities are better eliminated by the addition of 1% from a flux (detergent) to the binder. The high tension surface is thus decreased and the capillary forces could be highlighted to improve wettability (German, 1987; Campbell, 2003).

The infiltration is carried out in an electric furnace, after maintaining it 7 min at 1185°C, the mould is cooled at free air. The sintering temperature is selected in conformity with the size of the particles and their form and with the final specific composition. It is taken at 150°C beyond the fusion temperature of infiltrating. This temperature allows a good flow of the metal binder through the vertical channels, constituting the lengths of attack (supply). The distance is calculated according to the effectiveness of the tank (open deadhead) having a selected volume which will ensure the reduction of the shrinkage maiuly at the LP1 (W-Ni) binder-mixture interface.

Characterization

Microstructure

The samples are polished in the infiltration direction until completion with a 1 μm diamonds set. The microstructures are examined using a micrographic microscope NIKON EPIPHOT 300 and a scan electronic microscopy JEOL JSM 6830. The specific analyses as well as cartographies of nondissolved particles and phases resulting from solidification are established by dispersive energy spectroscopy (EDS). The identification of the phases is carried out by X-rays diffraction on Siemens D5000 diffractometer. For the metallographic study we use the acetic-nitric acid attached chemical solution.

HV30 Hardness Profiles and HV0.1 Microhardness

By filiation, profiles of Vickers hardness (HV30) are carried out over a 10 mm length, representing the depth of infiltration. HV0.1 microhardness is carried out using a PERSI DMÀ microdurometer by using 100 g load and a 15sec application time. Through the various layers of consolidated powders, it allows the much localized study of the phases resulting from the solidification of the binder, in particular in the vicinity of the WC, W and Ni particles.

RESULTS AND DISCUSSION

The homogeneity of the interfaces of the mixtures of powders will depend mainly on the mechanisms which can occur in the two stages of the infiltration. The observation of the obtained microstructure of the composites reveals the presence of two areas of interfaces in the infiltration direction (Fig. 3) the binder/LP1 area (due to the surplus of the binder during infiltration) and LP1/LP2 area.

The binder structure after solidification in the binder/LP1 area compared with that of the rough state corresponds to a dendritic structure without preferential orientations and presenting less segregation. The presence of nickel in this binder (Ni-bronze) contributes to the reduction of the segregation (reduction of solidification interval).

The DRX of binder in all samples reveals the solidification of a Cu solid solution (alpha) rich in substitute components on the level of the dendrite axes, of an eutectoid phase and a Sn rich phase (Cu_9NiSn_3) in interdendritic space. Indeed, the liquid enrichment with elements such Ni, Fe, Mn can even largely exceed the maximum composition of balance of the alpha phase (25% Sn). It is formed thus, during the solidification of the last traces of liquid, a phase out of balance which transform into eutectoid (Gupta *et al*., 1988).

The rearrangement of the solid particles contributes to the stacking of the structure. This phase will depend on the capillary force which itself depends on the wettability of the infiltrating mixture and on the Nickel which dissolves partially. The distribution of the Ni particles contributes to decrease the segregation in LP1 and LP2 areas. The persistent Nickel grain boundaries can be identified surrounded by pores resulting from the incomplete densification from generally round form.

For the considered cycle, there are certain relations between the physical properties of the powders and the behavior in infiltration, which become stronger for the fine powders. Thus, the granulometric distribution of the C_4 class seems to have the best tap densities than the other classes (mixture LP1: 8.9 g cm^{-3} for C_4 against 7.4, 7.2 and 7.3 g cm^{-3}, respectively for the classes C_1, C_2 and C_3). For the same proportion, form and distribution of Ni, the irregular shape of WC is better adapted to support a good densification classes (LP2 mixture: 9.9 g cm^{-3} for C_4 against 7.9, 7.7 and 8.2 g cm^{-3}, respectively for C_1, C_2 and C_3).

LP1/Binder Interface

At the infiltration temperature the liquid under gravity, wetting, causes capillary forces inducing the displacement of the particles (mass transport). The presence of large particles of W supports the

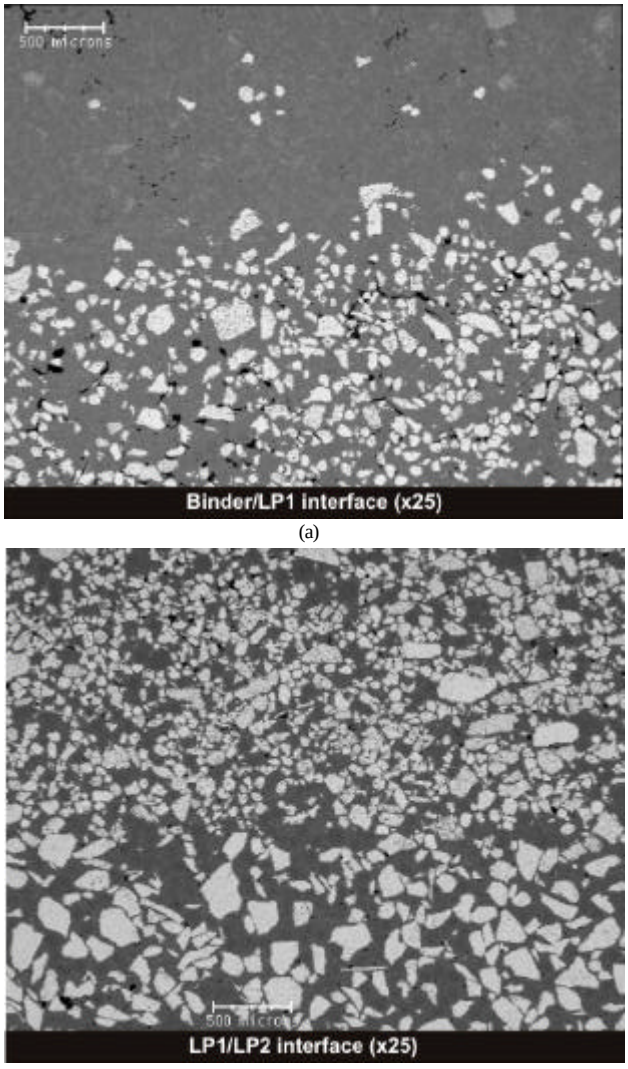

Fig. 3: MEB microstructure of the C_4 class composite infiltrated at 1185°C/7 min (a) W particles distribution and porosity to the binder/LP1 interface and (b) WC/W distribution in the LP1/LP2 interface

appearance of tunnels with broad capillarity for a better penetration (German, 1985). The private individual Ni fines are preferentially dissolved in the fusionned fluid. The gravity induced by excess of liquid cause microstructural and composition segregation (Upadhyaya, 2001; Upadhyaya and German, 2001; Wu *et al*., 2003; Delannay *et al*., 2005). The C_2 and C_3 classes are particularly sensitive to the segregation effect. Note also that under the infiltration conditions considered, the binder fusion led to a preferential dissolution of acute border and preserved them a round morphology, mainly in contact with the same nature particles (W/W) and thus an accommodation of the grains shapes (German, 1987; Upadhyaya, 2001; Hong *et al*., 2002).

Another aspect of the microstructural change is that the solid-liquid segregation lead to a rate presence of a significant solid and an adjacency in the lower part of the composite (Upadhyaya and

German, 2001). The solid-liquid segregation is more emphasis if the fluid fraction is important (C_3), with the preferential formation of a WC skeleton which can be allotted at the sintering stage in a solid state (Adorjan *et al*., 2006).

LP1/LP2 Interface

The presence of an separation area between the WC particles (Ni dissolved in the binder) of the LP2 powder being very visible, in particular, for the classes C_1 and C_2 (particles with fine granulometry). The tungsten morphology (polygonal form) is substituted by a rounded angles form, especially in contact with the particles of same nature (W/W).

The EDS concentration profile (Table 2) draws the distribution of main elements with a marked dissolution of the Ni particles under infiltration conditions. The Cu-Sn and Sn-Ni binary systems let suppose that the system is formed of liquid and α solid solution (Cu-Ni, Sn-Ni) at infiltration temperature (1185°C), for 20 wt% total proportion (Kingery, 1959).

In the areas with high nickel dissolution (Fig. 4), fragmentation, particularly of tungsten, is much more important. For a relatively short time of infiltration (7 min.) under the effect of the capillary forces, the nickel dissemination towards the interface of the W (WC) particles activates their dissolution (Kingery, 1959; Kwon and Yoon, 1981).

Table 2: Distribution of the main elements and variation of the microhardness to LP1/LP2 interface of C_4 class

		Elements (Wt. %)					
Positions	HV0.1	W	Ni	Cu	Sn	Mn	WC
A	458	100	0.00	0.00	0.00	0.00	-
B	267	0	24.28	68.16	04.00	03.56	0
C	219	0	49.59	45.14	01.53	03.74	0
D	163	0	100.00	0.00	0.00	0.00	0
E	167	0	43.29	51.44	02.15	03.12	0
F	228	0	21.75	64.41	09.80	04.04	0
G	322	0	30.34	37.96	27.79	03.91	0
H	215	0	48.23	46.21	02.08	03.48	0
I	362	0	27.09	66.76	01.43	04.72	0
J	1912	-	0.00	0.00	0.00	0.00	100

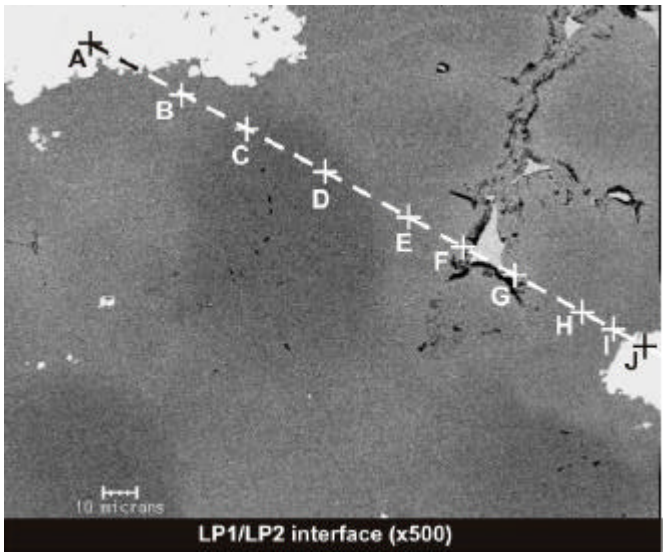

Fig. 4: The EDS concentration profile of the C_4 class (LP1/LP2 interface)

Porosity Evolution

The structural integrity of infiltrated body is closely associated to the microstructure. During the infiltration, the density of the solid is higher than that of the liquid and this one is higher than that of the pores (Lu *et al*., 2001). The liquid runs in the pores space of the packed mixtures. The size and the pore fraction, grow base of the sample upwards. For the same initial porosity in the sample, when the migration is slower than the closing way of pores, the liquid is faster and the solid migration traps the pores inside for a continuous sintering. This mechanism can be allotted to the loss of the contact between the grains of W/WC due to displacements of particles under the effect of the liquid pressure (revolved). Porosity in the classes C_3 and C_4 is more significant than in the two classes C_1 and C_2. Irregular pores form is observed in the interface, particularly, in the areas with strong presence of liquid (class C_3). A residual porosity is created during the infiltration process in the bottom part of sample due to liquid direction (upward to downward). While being based on the conventioual principle (Yoon and Huppmann, 1979a, b; Lee and Kang, 1998, Huppmann and Riegger, 1975; Yoon, 1979a), the densification by sintering in liquid phase, is closely related to the volumic liquid fraction. As the proportion of liquid is high, a complete density can be completed only by rearrangement of the particles (Xu *et al*., 1999).

Hardness Profile

Compared to the average hardness of binder (165 HV), it appears that hardness takes a growth evolution from top to bottom in the infiltration direction (Fig. 5). The partial dissolution of the nickel particles supports a maximum hardeness of the solid solution α and decreases the segregation. The formation of strong proportion zone with W/WC hard particles is due to compressing during the filling and the rearrangement under the effect of the significant liquid fraction. It considerably contributes to increase the hardness of the LP1L/P2 interface zone (except for the C_3 class). The large fall of hardness in this zone for the C_3 class is probably induced by the presence of a significant density due to closed pores. The highest level of hardness is however reached for the C_3 class, on the bottom grade of the samples. This is attributed to the contribution in hardness of tungsten carbide (HV0.1 of 1976) and to the presence of hardening elements (Ni, Mn) addition in the binder phases (Orban and Domsa, 1999; Uzunsoy and Chang, 2005; Kim *et al*., 2006; Srivatsan *et al*., 2004; Yang *et al*., 2005; Lumpkins, 1985).HV0.1 microhardness tests in the infiltration direction consolidate the effect of the hardening elements distribution in the various zones. The EDS cartography established in the LP1/LP2 interface zone (Fig. 6) shows clearly partial dissolution of the Ni particles and their distribution near the W (WC) hard particles. HV0.1 hardness of the non dissolved Ni grains corresponds to 163 average; it is about 220 in the zones close to Ni, whereas it exceeds 362 around the W (WC) particles.

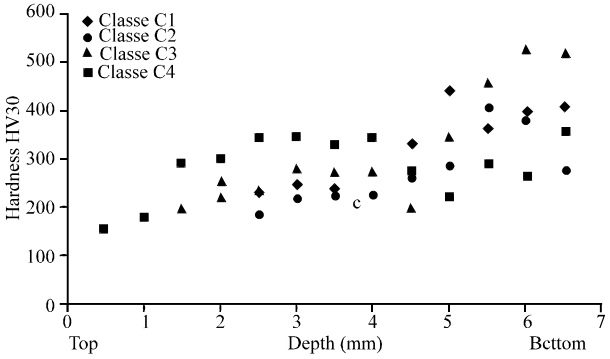

Fig. 5: HV30 hardness profile in the infiltration direction

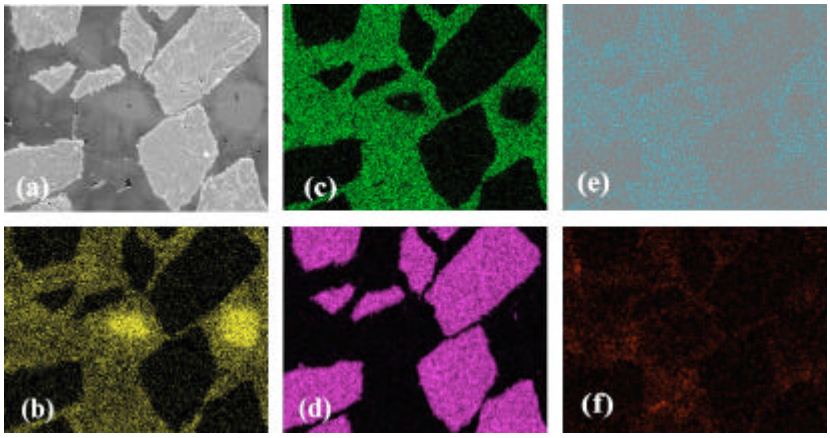

Fig. 6: EDS cartography established on the LP2 zone of C_4 class (a) MEB micrography of the LP2 class, (b), (c), (d), (e) and (f) represent the distribution of the chemical elements, respectively Ni, Cu, W, Sn and Mn

CONCLUSIONS

The control of the consolidation parameters, mainly the temperature and the infiltration time (1185°C/7 min) contribute to distribute homogenously the hardening elements in the various phases while avoiding interfacial precipitation.

The grannlometric distribution of the C_4 class seems to correspond to the best compromise for an optimal consolidation especially on the LP1/LP2 interface. The highest densification level corresponds to zones with high proportion out of WC (highest level of tap density). The free particles rearrangement under the gravity effect of the liquid and the accommodation of their contours under the precipitation effect of dissolved nickel; contribute at lot to the densification.

ACKNOWLEDGMENTS

This study was supported by Engineering and Science Materials Laboratory (USTHB) and Production Tools Division (PTD/ENSP-Algeria).

REFERENCES

Abd-Elwahed, M.A., 1999. Fabrication of metal matrix composite by infiltration process-part 2: Experimental study. J. Materials Processing Technol., 86: 152-158.

Adorjan, A., W.D. Schubert, A. Schön, A. Bock and B. Zeiler, 2006. WC grain growth during the early stages of sintering, Int. J. Refractory Metals and Hard Materials, 24: 365-373.

Ashurst, A.N., 1983. Copper infiltration of steel: Properties and applications. Powder Metallurgy, 139: 163-182.

Caceras, P.C., 2002. Effect of microstucture on the abrasive properties of infiltrated tungsten alloys. Materials Characterization, 49: 1-9.

Campbell, J., 2003. Casting. Elsevier Science, 143: 222-224.

Chong, S.Y., H.V. Atkinson and H. Jones, 1993. Effect of ceramic particle size, melt superheat, impurities and alloy conditions on threshold pressure for infiltration of SiC powder compacts by aluminium-based melts. Materials Sci. Eng., A173: 233-237.

Cook, A.J. and P.S. Werner, 1991. Pressure infiltration casting of metal matrix composites. Materials Sci. Eng., A144: 189-206.

Delannay, F., D. Pardoen and C. Colin, 2005. Equilibrium distribution of liquid during liquid phase sintering of composition gradient materials. Acta Materialia, 53: 1655-1664.

Domsa, S. and R. Orban, 1999. New developments in wear resistant hard materials processing by the powdered matrix infiltration with molten binder alloy. Proceedings, Euro PM 99 European conference on advances in hard materials production. Italie, pp: 199-204.

Eremenko, U.N., Y.V. Naidich and I.A. Lavrinko, 1970. Liquid Phase Sintering. Publishing, 7: 44-47.

German, R.M., 1985. Liquid Phase Sintering. Plenum Press, pp: 5-10, 119-122,160-162.

German, R.M., 1987. A Status report on liquid phase sintering. Powder metallurgy for full density products. Metal Powder Industries Federation, 8: 253-277.

Gille, G., J. Bredthauer, B. Gries, B. Mende and W. Heiurich, 2000. Advanced and new grades of WC and binder powder-their properties and application. Int. J. Refractory Matals and Hard Materials, 18: Issues 2-3, 87-102.

Goetzel, C.G. and A.J. Shaler, 1964. Mechanism of infiltration of porous powder-metallurgy parts. J. Metals, pp: 901-905.

Gupta, K.P., S.B. Rajendraprasad., D. Ramakrishna and A.K. Jena, 1988. The Cu-Ni-Sn system. J. Alloy Phase Diagrams, 4: 160-174.

Hong, S.H., H.J. Ryu and W.H. Baek, 2002. Matrix pools in a partially mechanically alloyed tungsten heavy alloy for localized shear deformation. Materials Sci. Eng., 333: 187-192.

Huppmann, W.J. and H. Riegger, 1975. Modelling of rearrangement processes in liquid phase sintering. Acta Metallurgica, 23: 965-971.

Kim, H.C., I.J. Shon, J.K. Yoon, J.M. Doh and Z.A. Munir, 2006. Rapid sintering of ultrafine WC-Ni cermets, Int. J. Refractory Metals Hard Materials, 24: 427-431.

Kingery, W. D., 1959. Densification during sintering in the presence of a liquid phase. Theory J. Applied Phys., 30: 301-306.

Kumar, S. and J.P. Kruth, 2007. Effect of bronze infiltration into laser sintered metallic parts. Materials and Design, 28: 400-407.

Kwon, O.J. and D.N. Yoon, 1981. Closure of isolated pores in liquid phase sintering of W-Ni. Int. J. Powder Metall Tech., 17: 127-133.

Lee, S.M. and S.J.L. Kang, 1998. Theoretical analysis of liquid-phase sintering: Pore filling theory, Acta Material., 46: 3191-3202.

Lumpkins, E.R., Jr, 1985. A theoretical review of the copper infiltration of PM components. Powder Metallurgy Int., 17: 120-123.

Miroud, D., S. Lebaili and S. Hamart-Thibault, 2001. Interface studies in metallic matrixes WC-W_2C-Ni and W-Ni infiltrated by the Cu-Sn-Ni-Mn as binder in 'SILP' process. Proceedings, Euro PM 99 European Conference on Advances in Hard Materials Production, Nice Nov., pp: 67-75.

Orban, R. and S. Domsa, 1999. Metallic binder for diamond tool production using synthetic diamond. Proceedings, Euro PM 99 European Conference on Advances in Hard Materials Production, Italie, pp: 65-70.

Lu, P., Xu Xiaoping, Y. Wuwen and R.M. German, 2001. Porosity effect on densification and shape distortion in liquid phase sintering. Materials Sci. Eng., A318, 111-121.

Shaler, A.T., 1965. Theoretical aspects of the infiltration of powder metallurgy products. Int. J. Powder Metallurgy, 1: 3-14.

Shatov, A.V., S.A. Firstov and I.V. Shatova, 1998. The shape of WC crystals in cemented carbides, Materials Sci. Eng., A242, 7-14.

Srivatsan, T.S., R. Woods, M. Petraroli and T.S. Sudarshan, 2004. An investigation of the influence of powder particle size on microstructure and hardness of bulk samples of tungsten carbide. Int. J. Refractory Matals and Hard Materials, 37: 523-528.

Thibault, S.H., C. Et. Allibert and W. Tillman, 1999. Phase constitution of Cu77Sn8Ti14Zr1 as binder for diamond tools. Proceeding of International Workshop on Diamond Tool Production, EURO PM, Turin, pp: 57-64.

Upadhyaya, A., 2001. Processing strategy for consolidating tungsten heavy alloys for ordnance applications, Materials Chem. Phys., 67: 101-110.

Upadhyaya, A. and R.M. German, 2001. Gravitational effects during liquid phase sintering. Materials Chem. Phys., 67: 25-31.

Uzunsoy, D. and I.T.H. Chang, 2005. The effect of infiltrant choice on the microstructure and mechanical properties of Rapidsteel. Materials Lett., 59: 2812-2817.

Wannasin, A.J. and M.C. Flemings, 2005. Fabrication of metal matrix composites by a high-pressure centrifugal infiltration process. J. Materials Processing Technol., 169: 143-149.

Wu, Y., R.M. German, B. Marx, R. Bollina and M. Bell, 2003. Characteristics of densification and distortion of Ni/Cu liquid-phase sintered tungsten heavy alloy. Materials Sci. Eng, A344: 158-167.

Xu, X.A., Upadhyaya, R.M. German and R.G. Iacocca, 1999. The effect of porosity on distortion of liquid phase sintered tungsten heavy alloys. Int. J. Refractory Metals Hard Materials, 17: 369-379.

Yang, G.R., Y. Hao, W.M. Song and Y. Ma, 2005. An investigation of the structure and properties of infiltrated layer on the surface of copper alloy. Materials Sci. Eng., A399: 206-215.

Yoon, D.N. and W.J. Huppmann, 1979a. Grain growth and densification during liquid phase sintering of W-Ni. Acta Metallurgica, 27: 693-698.

Yoon, D.N. and W.J. Huppmann, 1979b. Chemically driven growth of tungsten grains during sintering in liquid nickel. Acta Metallurgica, 27: 973-977.